Renewable Energy 134 (2019) 538–549

Contents lists available at ScienceDirect

Renewable Energy

journal homepage: www.elsevier.com/locate/renene

Multi-figure of merit optimization for global scale sustainable power systems

Hussein M.K. Al-Masri [a, *], Ahmad AbuElrub [b], Abdullah A. Almehizia [c], Mehrdad Ehsani [d]

[a] Department of Electrical Power Engineering, Yarmouk University, Jordan
[b] Department of Electrical Engineering, Jordan University of Science and Technology, Jordan
[c] National Center for Technologies of Electrical Energy Systems, King Abdulaziz City for Science and Technology, Saudi Arabia
[d] Department of Electrical Engineering, Texas A&M University, College Station, USA

ARTICLE INFO

Article history:
Received 4 January 2018
Received in revised form
8 November 2018
Accepted 12 November 2018
Available online 15 November 2018

Keywords:
Hybrid wind/PV power system
Sustainable energy systems
Techno-economic
Mitigation of greenhouse gases (GHG)
Genetic algorithm
NSGA

ABSTRACT

The main goal in this paper is to supply a national load by multiple renewable power connections to utility grid at different geographic locations. The national load demand of the country of Jordan is supplied in this case study by finding the optimal configurations and locations (near cities). Cities of higher potential for wind and/or photovoltaic (PV) energy location are selected for connecting to renewable power. The annual system cost of energy (ASCE) for this optimized renewable energy system is shown to be 32.57% less than the conventional grid energy price. Further, the Carbon Dioxide (CO_2) emissions are reduced by 80.13%. These are excellent indications for the feasibility and environmental benefits of retrofitting conventional grid with renewable power in developing countries. Multi-figure of merits (MFOM) based on a Nondominated Sorting Genetic Algorithms (NSGA) optimization cases are investigated which include annual emission indicator (AEI), ASCE, levelized cost of energy (LCOE) and renewable penetration (RP). Results are either two dimensions (2D) or three dimensions (3D) Pareto frontier, where various competitive non-dominant solutions exist. A sweet spot selection (triple-S) procedure is proposed to help select the best point in the two (figure of merits) FOMs Pareto frontier to have both environmental and feasible solutions.

© 2018 Elsevier Ltd. All rights reserved.

1. Introduction

Electricity is considered the most flexible form of power known to humankind and one of the most common energy delivery forms used in residential, industrial and commercial applications [1]. Although the fossil fuels have served humanity for nearly two centuries the reserves of coal, oil and natural gas will not last indefinitely by their very nature. Therefore, new sources of energy are needed, such as the renewable sources, which are considered the long term solution to energy needs [2]. However, it can be hard to justify the cost of the renewable energy when the oil prices are so low. The falling of oil prices, since 2014 has had three main consequences: Financial problems in the worldwide oil industries, reduction of investment in the conventional fossil fuel resources, and employee lay off in oil companies. On the other hand, investments in renewable energy projects are on the rise. Wind and solar photovoltaic energy resources are considered most favorable because they are non-depletable, ubiquitous and essentially nonpolluting. Numerous studies to optimize the single figure of merit, FOM, problem have been reported in the literature. In Ref. [3], the authors used the hourly data for the whole year for a house in Okinawa, Japan. Then, they used genetic algorithms, GA, to minimize the single figure of merit (FOM) problem of total cost that includes initial cost and operational and maintenance costs (OMC). Those authors did a type of approximation, which affects the system component sizing. In the wind turbine (WT) modeling, they assumed a linear behaviour between the cut-in and the rated wind speed, which is simple but not precise. Thus, an optimal configuration of renewable generating system was obtained. But, the total cost is more reasonable when obtained by using the GA method. In Ref. [4], the authors performed an optimization process on a stand-alone hybrid wind-solar system with backup battery banks. The two FOMs were the total annualized cost (TAC) and the loss of power supply probability (LPSP). The decision variables were number of PV panels (PVs), number of wind turbines (WTs),

* Corresponding author. Yarmouk University Electrical Power Engineering Department, Shafiq Irshidat st, Irbid, 21163, Jordan.
E-mail address: h.almasri@yu.edu.jo (H.M.K. Al-Masri).

https://doi.org/10.1016/j.renene.2018.11.053
0960-1481/© 2018 Elsevier Ltd. All rights reserved.

Nomenclature

FOM	Figure of merit
ASCE	Annual system cost of energy
LCOE	Levelized cost of energy in $/kWh
TNPC	Total net present cost in $
CC	Capital cost
RC	Replacement cost
OMC	Operation and maintenance cost
SC	Salvage cost
RP	Renewable penetration
AEI	CO_2 annual emission indicator
MFOM	Multi-figure of merit
GA	Genetic Algorithm
NSGA	Non-dominated sorting GA
V_{ci}	Cut-in wind speed value in m/sec
V_{rated}	Rated wind speed value in m/sec
V_{co}	Cut-out wind speed value in m/sec
AEE	Annual energy extracted (in kWh)
P_{WT}	Output power of a wind turbine
P_{RWT}	Rated power of a wind turbine
ρ	Air density in kg/m^3
ρ_o	Air density at sea level (1.225 kg/m^3)
D_R	Turbine rotor diameter in (m)
T	Temperature in Kelvin (K)
H	Altitude above sea level in (m)
g	Acceleration due to gravity (9.80665 m/s^2)
M	Molecular weight of dry air (0.0289644 kg/mol)
R	The ideal gas constant (8.31432 N.m/(mol·K))
A_{WT}	Single WT swept area in m^2
N_{WTrows}	Number of wind turbines rows
A_{PV}	Area of a PV module in m^2
N_{PV}	Number of PV panels
N_{PVrows}	Number of PV rows
P_{PV}	Output power of a PV module
P_{RPV}	Rated power of a PV module
RI	Global radiation incident on PV module (kW/m^2)
TC_P	Maximum power temperature coefficient (%/°C)
TC	Module cell temperature in °C
$T_{ambient}$	Ambient temperature in °C
T_{NOCT}	Nominal operating cell temperature in °C
L_{PV}	Length of a PV panel in m
W_{PV}	Width of a PV panel in m
d_{min}	Minimum spacing between the PV panels
β	Module tilt angle

number of batteries, slope angle of the PV panel and WT installation height. The objective was to find the best compromise between TAC and LPSP. The results showed that as LPSP decreases, TAC increases. For a 1% desired LPSP, TAC of hybrid wind-PV system is $10,600 which is less than $11,145 for PV only and $16,889 for wind only configuration.

However, most of the reviewed literature investigates a single point connection to the utility grid with a given load demand, wind speed and insulation data at one location. However, this paper addresses the important problem of multipoint connection for integration of renewable power plants to any national grid system. The case study of Jordan national grid is used to illustrate theoretical modeling and mathematical optimization techniques that can also be used for other countries with differing specifics. We have combined wind and PV, multi-point connection with considerations of resource availability and grid capacity, to optimize the cost of electricity to the consumer, justify the life time investment by the country based on cost and hybridization optimization. The problem of multi-point grid connection, shown in this paper, is not found clearly in the literature.

For instance, in Ref. [5], an optimization framework for the layout and location selection of offshore wind farm in the United Kingdom is proposed. The optimization procedure is based on life cycle cost analysis which includes many cost phases starting from redevelopment and consenting cost to decommissioning and disposal cost. The Non-dominated Sorting Genetic Algorithm (NSGA-II) is employed to minimize the overall cost of the system. The authors of [6] presented an application of data analysis of the electricity production in order to calculate different performance indicators which are the primary energy factor, CO_2 emission factor, the renewable energy share. The results showed a significant variability of the indicators, which in turn show the importance of an accurate knowledge of operational parameters for future smart grids. In Ref. [7], two multi objective evolutionary algorithm were used to find the optimal layout of offshore wind farms and the results were compared. The Multi-Objective Gene-pool Optimal Mixing Evolutionary Algorithm (MOGOMEA) and the NSGA-II were employed. The case study showed that the MOGOMEA outperformed the NSGA-II in the problem size and the constraint handling techniques. A new multi-objective optimization transmission expansion planning algorithm incorporating wind farm generation was presented in Ref. [8]. The NSGA-II was used to solve the optimization problem and the final optimal solution selected based on a fuzzy decision-making approach. In Ref. [9], a study to find the optimal selection of wind turbines based on the cost of energy and the local wind condition was conducted. This study highlighted the need for a framework to deal with such complex problems where the optimal decision is needed.

This paper illustrates our concept of “local solutions for a global problem”, by having a unique definition of the design optimization problem. In our case study, the national load demand of the country of Jordan will be supplied by finding the optimal configuration at six locations (or cities). Only those cities with high potential for wind and/or PV power is used to install wind farms and/or PV arrays. This means that some cities may not be selected for the time being because the national load is supplied by the higher potential locations (See Table 7). An optimization approach is used. In the first single objective optimization problem, the objective function (or FOM) is the ASCE. In the second optimization multi-objectives problem (or MFOM), the objective functions are AEI, ASCE and LCOE. Further, the single FOM and MFOM optimizations are used to find the optimal wind and/or PV configurations for multiple high potential cities in order to supply the national load demand for method validation study [10]. The network constraints and power flow limits are assumed to be met by setting an installation area cap limit for each city (See Table 8). This makes the model practical for most existing security considerations. Fig. 1 shows a Google Earth map for the country of Jordan, where the area for the six candidate cities of high potential for wind and solar power are indicated. Also, see Table 1.

Jordan is a non-oil producing country, where most of the fuel is imported. It has one of the highest dependencies on foreign energy resources in the world. Around 96% of Jordan's energy comes from imported natural gas and oil. This constitutes a significant financial burden on the Jordanian national economy by consuming a significant fraction of the gross domestic product (GDP). This has

motivated the decision makers in Jordan to plan investments of $15 billion in renewable and nuclear energy [10]. Therefore, considerable research effort is being committed to renewable energy.

2. Multi-point data acquisition & preparation

In this section, the data needed to solve the multi-point grid connection problem, will be presented.

2.1. Data sources

The load demand values were obtained using a supervisory control and data acquisition (SCADA) system operated by the National Control Centre of the National Electric Power Company [11], which is responsible for transmission of electrical power in Jordan. The wind speed and solar insolation data for six candidate sites are obtained by referring to the Energy Centre of the Jordan Royal Scientific Society [12], which is an accredited centre to measure and prepare data needed for renewable energy studies in Jordan. The sources of cost data for the system components and grid are discussed in details in Ref. [13].

Fig. 1. Wind & PV candidate cities in Jordan.

2.2. Data description

Equation (1) is employed to compute the WT shaft output power captured by the blades. Jordan national load profile in 2014 is shown in Fig. 2. Note that, the load data is gained by the SCADA system every 60 min for the entire year of 2014.

In order to have a sense of the wind and solar power potential in these sites, the annual average values for each candidate city are shown in Table 1. The reason for selecting those candidate cities is that either they have a good grid infrastructure for wind farms or high average annual wind speeds in excess of 6–7 m/s, according to the wind atlas of Jordan [14]. The geographically available area at each city (that is neither inhabited nor planted) must be available in order to install wind farms and/or PV arrays. The multipoint grid connection component costs are shown in Table 2. The capital cost (CC) is the component cost plus the installation cost [13]. Note that, the CC or the OMC of WT and PV panel include the converter cost.

The existing grid capacity is equal to the national load demand. Whenever the renewables cannot satisfy the national load demand, the power deficit is supplied by the conventional generators, with the grid purchased price shown in Table 2.

3. Mathematical modelling and investigation

In this section, the mathematical models of the WT and PV module output power, footprint areas of the wind farm and PV array are presented. Further, system performance indicators such as annual system cost of energy (ASCE), annual emission indicator (AEI) and renewable penetration (RP) are explained.

3.1. Modeling of WT output power

Equation (1) is employed to compute the WT shaft output power captured by the blades. It is used to precisely model the WT by accounting for parameters affecting the output power, such as

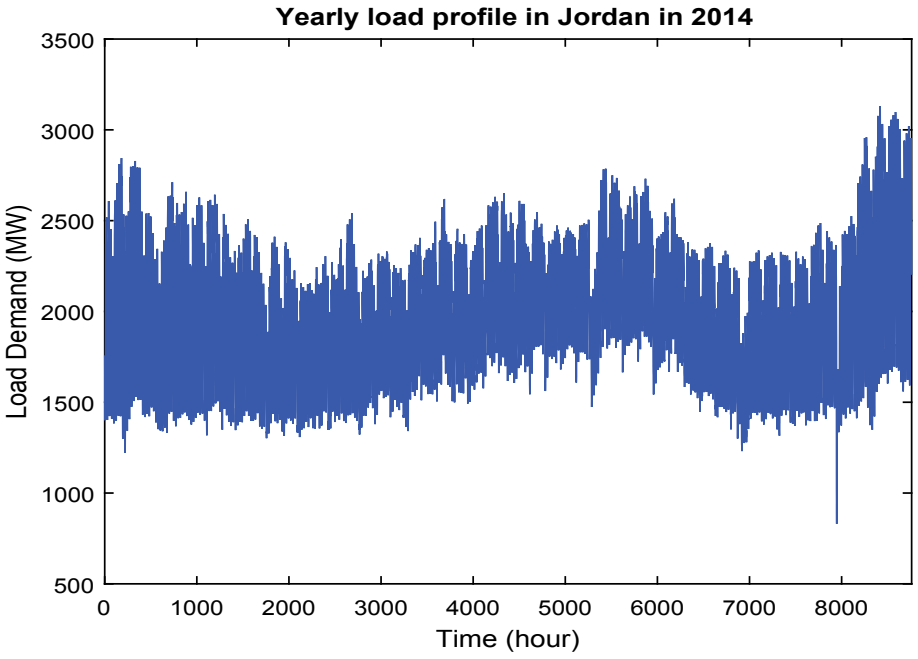

Fig. 2. National hourly load profile in Jordan in 2014.

Table 1
Multi-point connection candidate cities information.

Candidate Cities	Elevation a.s.l (m)	Geographic Available Area Cap (km^2)	Average radiation in 2015 ($kWh/m^2/day$)	Average Wind Speed in 2015 (m/s)
Ramtha-JUST	591	28.3148	5.5533	4.88
UmEjmal-LH	750	7.3338	5.7617	6.10
Ibrahimyya	1021	3.7637	5.5533	7.17
Alreesha2-LH	876	470.2879	5.7617	7.03
Maan-LH	1196	83.16	6.0308	5.92
Aqaba5	139	67.3257	6.1217	7.33

Table 2
Multi-point grid connection component costs.

	PV Module	Wind Turbine	Converter
CC	2770 $/kW	2098$/kW [13]	Included
OMC cost	10$/year	20.98$/kW/yr	Included
RC	0	2098$/kW	300$/kW
Grid energy price	0.14043 $/kWh		
Life Time	25 years	20 years	15 years
Project Life Time	25 years		

elevation above sea level (a.s.l), air temperature, in addition to wind speed and WT power coefficient. Wind power law in Ref. [13] is used to convert the anemometer measured hourly wind speeds into the speeds at the WT hub height in order to substitute in (1).

$$P_{WT} = \begin{pmatrix} 0 & 0 < v < v_{ci} \\ \frac{\Pi}{8} D_R^2 \rho v^3 Cp & v_{ci} < v < v_{rated} \\ P_{RWT} & v_{rated} < v < v_{co} \\ 0 & v > c_{co} \end{pmatrix} \quad (1)$$

C_p is the WT power coefficient [13,15]. It is simply defined as the ratio of turbine power to the wind power, and it has a constant maximum value in the range between the cut-in and rated wind speed values (V_{ci} and V_{rated}) [16]. The constant ρ is the air density computed in kg/m^3 as Equation (2) shows, which is derived and discussed in details in Ref. [17]. This model includes many exogenous parameters, which are set and combined to accurately model the real value of air density above sea level. This includes air density at sea level (i.e. 1.225 kg/m^3), altitude above sea level (H in m), acceleration due to gravity (9.80665 m/s^2), molecular weight of dry air (0.0289644 kg/mol), ideal gas constant ((8.31432 N.m/(mol·K))), the temperature lapse rate (L = 0.0065 °C/m) [18]. T_o is temperature at sea level (288 K) [18], is used in Equation (3) to calculate the temperature in K at the given height above sea level.

$$\rho = \rho_o \times \left(1 - \frac{LH}{T_o}\right)^{\frac{gM}{RL}} \times \frac{T_o}{T} \quad (2)$$

$$T = T_o - LH \quad (3)$$

As the elevation and temperature increase, ρ decreases. This density reduction makes the rated WT speed to be shifted to the right of the WT output power curve (WTC) [19]. Therefore, the area of the WTC is reduced. This highly affects the WT annual extracted energy, which affects the size and cost of the wind farm.

Table 3
"GE 1.5SLE" wind turbine.

Parameter	P_{RWT}	D_R	V_{ci}	V_{rated}	V_{co}	Hub height
Value (Unit)	1.5 MW	77 m	3.5 m/s	14 m/s	25 m/s	80 m

The WT energy is computed by multiplying the time step of 1 h with the WT output power (P_{WT}) shown in (1). Table 3 shows specifications of the selected WT.

3.2. Footprint of the wind farm

To compute the area of the entire wind farm, it is very important to specify the spacing between the WTs. It is 3.5 times the wind turbine rotor diameter (D_R) within the row and 10 times D_R between the rows of the wind farm [20]. These spacings are important for mitigating the turbulence due to the rotation of the blades. The minimum rectangular geographic area of the wind farm (A_{WTs}) is obtained by using equation (4). Here, N_{WTrows} is the number of rows in a rectangular wind farm.

$$A_{WTs} = D_R^2 \left(35 N_{WT} - 31.5 \frac{N_{WT}}{N_{WTrows}} + 22.5\right) \quad (4)$$

3.3. Modeling of PV module output power

The global solar radiation incident on the surface of the PV array is obtained for each candidate city in Table 1. The output PV power is computed by Equation (5) [21]. Annual energy extracted (AEE) is computed by multiplying the time step with the PV output (P_{PV}).

$$P_{PV} = P_{RPV} \times \frac{R_I}{R_{STC}} \times [1 + (T_C - T_{STC}) TC_P] \quad (5)$$

The PV system is generally rated at standard test conditions (STC) ($T = 25\,°C$, $R_{STC} = 1\,kW/m^2$). The ratio of (R_I/R_{STC}) is called normalized de-rated radiation. In practice, the operating conditions may be different, i.e. the temperature could be higher or the insolation could be lower. So, it is very important to know the PV system operating cell temperature, in order to calculate the actual output from the PV system. T_{NOCT} is defined at insolation of 0.8 kW/m^2 and air temperature of 20 °C. Experimentally, it is found that the best formula describing the PV cell temperature (T_C) estimate is as shown in Equation (6) [22].

$$T_C = T_{ambient} + (T_{NOCT} - 20) \times \frac{R_I}{800} \quad (6)$$

Table 4 shows the specifications of the selected PV module. Here, fill factor measures the quality of PV module, and helps select the suitable PV panel available on the market [23].

Table 4
"VBHN240SA11" PV module.

Parameter	P_{RPV}	L_{PV}	W_{PV}	TC_P	T_{NOCT}	η	FF
Value (Unit)	240 W	1.58 m	0.798 m	−0.3%/°C	48.3°C	21.6%	78.55%

3.4. Footprint of the PV array

Self-shading occurs if the rows of the PV arrays are too close to each other. However, if the rows are spaced too far apart, while the self-shading will be reduced, but the land cost will increase. So, an optimum spacing ($d_{\min}$) between the PV panels should be adhered to in order to prevent self-shading [24] as depicted in Fig. 3.

The PV array should be installed for no self-shading on the shortest day of the year. In the Northern hemisphere, December 21st (Winter Solstice) at 12 p.m. is the time when the Sun has the minimum elevation as can be found using a sun path diagram [24]. Equation (7) was developed to compute the minimum geographic footprint of the entire PV array. Here, N_{PVrows} is the number of rows in a rectangular PV array and L_{PV} and W_{PV} are the length and the width of the PV module in Table 4.

$$A_{PVs} = [(N_{PVrows} - 1)d_{min} + L_{PV}\cos\beta]\frac{W_{PV}N_{PV}}{N_{PVrows}} \quad (7)$$

3.5. System performance indicators

There are several system indicators, that can be used to evaluate the performance of renewable energy systems in terms of economic feasibility and environmental issues, as shown below.

3.5.1. The ASCE

Equation (8) is used to compute the cost of energy produced by the on-grid renewable energy system, ASCE, to supply the national load demand in Fig. 2.

$$ASCE = \frac{Annual\ System\ Cost\ (\$)}{Total\ Energy\ served\ (kWh)} \quad (8)$$

Here, ASCE is the FOM that will be optimized using the GA or NSGA. Supplying the national load from the wind/PV system is given priority, with a LCOE price. Thus, any power deficit will be supplied with the grid power, at its price. The LCOE mathematical formulation is explained in detail in another paper by the present authors [13]. There, by building a discounted cash flow (DCF) for the system components is used to compute the total net present cost (TNPC) in $. The DCF includes the cost components of CC, OMC, RC and salvage cost (SC). In this paper, Equation (9) is developed to compute the SC. The SC is the cost of any component in the renewable system at the end of the project lifetime. The SC has a direct relationship to the RC as well as to the remaining lifetime of the component with respect to its manufacturer specified lifetime. It is necessary to compute how many times (n) the component (WT, PV or converter) is replaced during the project lifetime. Then, the remaining time of the component is computed by multiplying the ceiling value of (n) with the component lifetime. The SC is computed using (9).

$$SC = RC \times (ceil[n] - n) \quad (9)$$

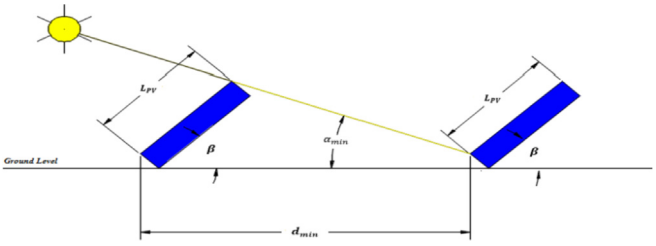

Fig. 3. Typical layout spacing of a PV array.

3.5.2. The AEI

Fig. 4 shows that the impact on the ecological system comes mainly from CO_2 emissions, which constitutes 76% of the global GHG [25,26].

Therefore, Therefore, the AEI is modelled in the design tool to indicate the quantity of CO_2 emitted by each unit of energy purchased from the grid if renewables cannot fully supply the national load demand. In this paper, the AEI is measured in megatons of CO_2/year. It is computed by multiplying the CO_2 Emission Factor (EF in $kgCO_2$/kWh) by the total annual grid fossil fuelled energy purchases. Emission factors have great impacts on the estimation results. The EF is estimated to be 0.580548 $kgCO_2$ per kWh based on the emission reports, standards and international institutes such as Institute for Global Environmental Strategies (IGES), which were used to estimate the emission factor in Jordan [26,27].

3.5.3. The RP

The RP in Equation (10) is the ratio of the renewable energy produced (E_{ren}) to the total energy produced (E_{tot}).

$$RP = \frac{E_{ren}}{E_{tot}} \quad (10)$$

Here, RP is modelled to give the produced renewable energy. It is used to compare the optimization trade-off relationships among other FOMs, such as the ASCE, LCOE and the AEI. It may be called an environmental impact indicator. Here, E_{ren} is produced by renewables and E_{tot} is the total energy produced by the renewables and

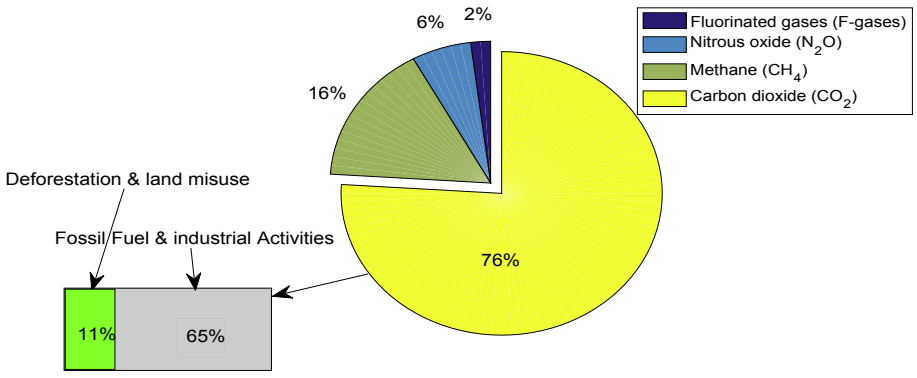

Fig. 4. Global GHG emissions' percentages.

the utility grid combined.

4. Overview of the genetic algorithms

Designing hybrid renewable systems becomes more complex because of the non-linear characteristic of the system components, the stochastic availability of the renewable energy resources (i.e. solar and wind) and the large number of the design optimization constraints and decision variables [28]. In this paper, two investigations are presented. First, GA to optimize a single FOM. The Initial population of solutions is randomly selected and tested in using a single FOM. In the selection operator, solutions are selected from the population according to their FOM. The crossover exchanges subparts of two solutions. Two numbers are selected and exchanged in the mutation operator. It helps get the global solution, avoiding the local solutions [29].

Second, the presence of MFOM problems includes a set of optimal results called Pareto frontier optimal solutions. Here, NSGA is one of the methods used to solve such a problem. Fig. 5 shows the NSGA flowchart operators applied to solve our MFOM multi-point connection problem.

The NSGA starts optimizing by randomly generating an initial population. Then, it discovers the trade-off solutions from the MFOM multi-connection problem. Then, the distance crowding is computed. This is defined as the distance between two adjacent solutions on each side of this solution [30]. Moreover, these non-dominant Pareto fronts are sorted from the highest rank FOM to the lowest rank FOM [31]. Thereafter, the natural GA inspired operators of Selection, Crossover, and Mutation are applied to obtain a new set of solutions added to the old set, making a new generation. Thereafter, Pareto non-dominance check for this generation provides and export the set of solutions called non-dominant, or trade-off solutions, based on the Pareto fraction. The Pareto fraction controls the elitism in the NSGA [32]. In the final set, there is no solution that is strictly better than any other solution.

5. Performance results and discussion

In this section, the results for the problem of the multi-point connection of a renewable power system to the utility grid of Jordan are presented, as our case study. This was done by developing an optimization criteria and design tool by applying the GA and NSGA to find the optimal and feasible solutions of our multi-point-connection problem.

5.1. Filling order of the candidate cities

The GA operators are applied to optimize the number of renewable units to supply the national load of Jordan. The criteria of the filling order, to allocate renewable WTs and PVs in each city, is done by computing the AEE from a single renewable unit installed in each candidate city as shown in Table 1. Table 5 shows the candidate cities arranged with respect to the solar and wind potential.

5.2. Single FOM solution satisfying national load

Fig. 6 shows how the GA looks for the optimal ASCE solution by figuring out some candidates and then selecting the optimal one, which is the best fitness feasible value. For each generation, there are two values: best fitness (dots in Fig. 6) and mean fitness (circles in Fig. 6). Fig. 6 shows how the optimizing process converges. The

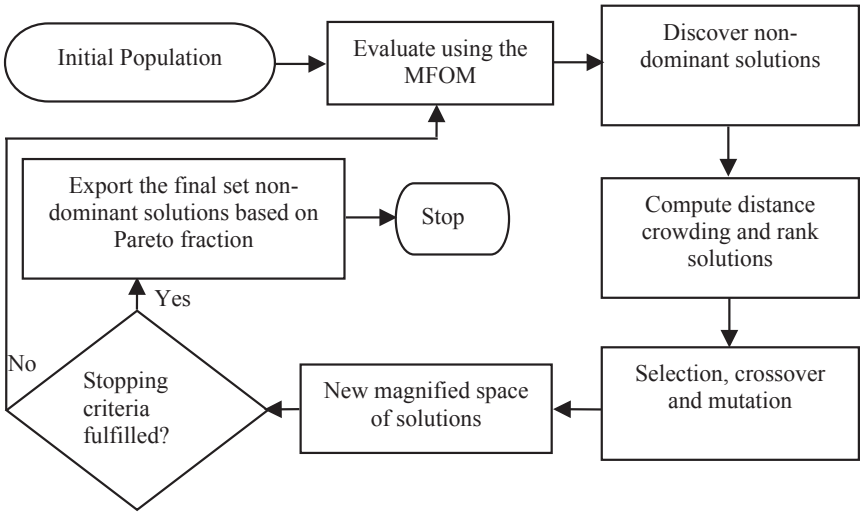

Fig. 5. NSGA operators for a MFOM.

Table 5
Renewables filling order.

WT Filling Order		PV Filling Order	
Arranged Candidate Cities	AEE of one WT unit (GWh)	Arranged Candidate Cities	AEE of one PV unit (kWh)
Aqaba5	5.9665	Aqaba5	480.3399
Ibrahimyya	5.4995	Maan-LH	473.3330
Alreesha2-LH	5.3680	UmEjmal-LH	452.4668
UmEjmal-LH	4.0687	Alreesha2-LH	452.4668
Maan-LH	3.6442	Ramtha-JUST	436.2410
Ramtha-JUST	2.2990	Ibrahimyya	436.2410

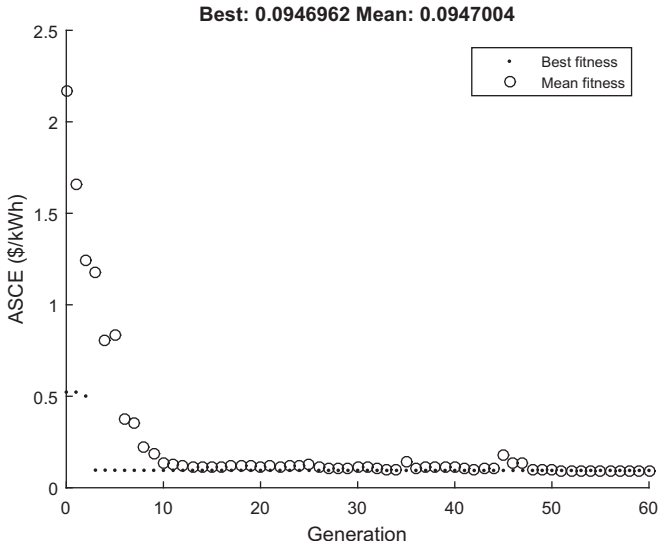

Fig. 6. GA optimization of ASCE as the FOM.

best FOM dot values of the last generations become the inside the mean circle values. Afterwards, the GA optimizes the ASCE as a single FOM with a value of 0.0946962$/kWh, which is 32.57% less than the Jordanian conventional utility grid energy purchased price. This is an excellent indication of the feasibility of this system, when practically implemented.

Moreover, Fig. 7 shows the genealogy of the GA individual solutions, which depicts children of mutation, crossover and elitism for sixty generations, each with a two-hundred population. To supply the national load of Jordan, the number of renewable unit decision variables are optimized to be 2079 for WTs and 129,362 for PVs. The specifications of the selected WT and PV module are shown in Tables 3 and 4, respectively. The optimized system for supplying the national load of Jordan is a hybrid wind/PV/grid configuration with the details shown in Table 6.

Table 6
Single FOM satisfying the national load.

ASCE in $/kWh	0.0946962
LCOE in $/kWh	0.058212
TNPC in billion $	8.713857
RP in %	59.49817
AEI (Megatonne/year)	4.576
Grid purchases (TWh/year)	7.8823

The Global Carbon Atlas in Ref. [33] shows that the CO_2 Emissions in Jordan in 2014 is 23MtCO_2 for a total number of population of 7,416,083. Therefore, our designed system will reduce the AEI by 80.13% as shown in Table 6. This is another excellent indication for the environmental benefit after solving the multi-point connection problem in Jordan.

The minimum areas required to accommodate the optimized value of WT and PV units have been computed to be 301.6853 km^2 and 196,158.1 m^2, respectively. These areas require more than one city (See Table 1) for their installation. Therefore, various renewable configurations are expected for each city based on their potential of renewable energy resources.

5.3. Multi-point solutions using GA

Table 7 shows that the hybrid wind/PV is the optimal and the feasible configuration in Aqaba5 site. Moreover, the wind only configuration is the best to be installed in the 2nd and the 3rd cities. The PV only configuration is the optimal in the MaanLH site. There is no need to install renewables in the last two cities for the current

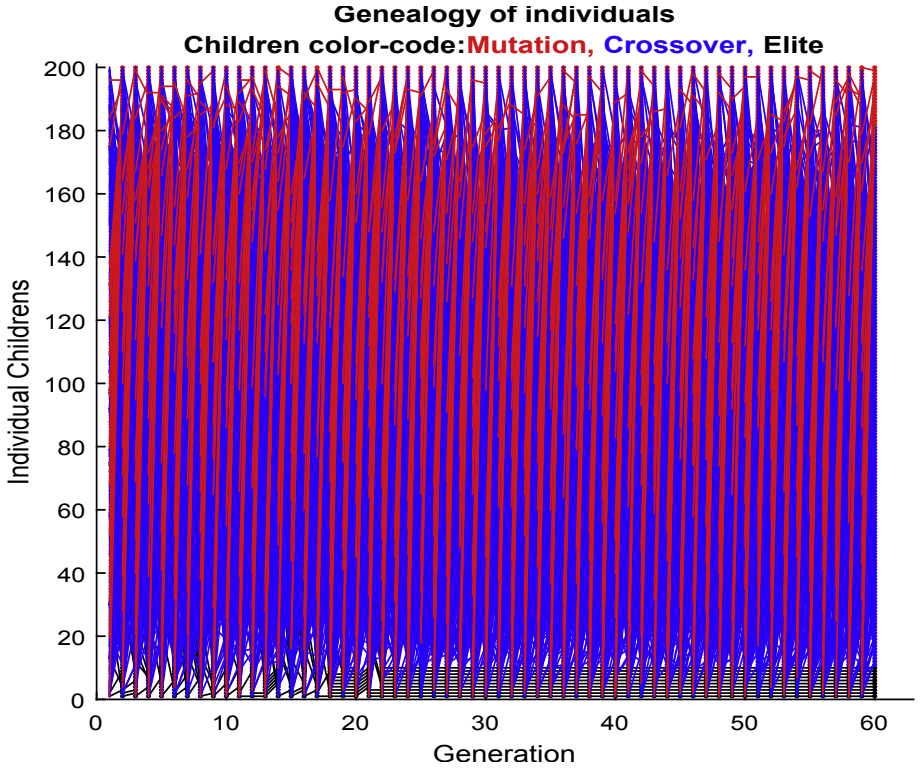

Fig. 7. Genealogy of individual children.

Table 7
Optimal configurations of multi-point connection.

Candidate Cities		On-Grid System Type	Number of Units	
#	Name		WTs	PVs
1	Aqaba5	Hybrid Wind/PV	590	59696
2	Ibrahimyya	Wind Only	34	0
3	Alreesha2-LH	Wind Only	1455	0
4	Maan-LH	PV only	0	69666
5	UmEjmal-LH	No need for the current national load	0	0
6	Ramtha-JUST		0	0

Table 8
Optimized values: sharing percents, dedicated and occupied area.

City #	Optimized sharing (%)		Dedicated area (km^2)		Occupied area (km^2)	
	WTs	PVs	WTs	PVs	WTs	PVs
1	99.86	0.14	67.23	0.0909	67.18	0.0908
2	99.55	0.45	3.75	0.02	3.72	0
3	82.11	17.89	386.16	84.13	211.04	0
4	34.06	65.94	28.32	54.84	0	0.10529
5	75.70	24.30	5.55	1.78	0	0
6	34.74	65.26	9.84	18.48	0	0

national load in Fig. 2. However, in the future it can be foreseen that the load will grow. Further, the GA specifies the WT sharing percentage (SPs) as six decision variables for each candidate city, as shown in Table 8. These are used to compute the dedicated minimum WT area for each candidate city. The dedicated area of WTs or PVs is less than the geographically available area cap shown in Table 1. As expected, the cities with high potential for wind or PV energy would have the highest share of renewable areas. Thus, Aqaba5 has the highest annual wind speed and the highest annual radiation (See Table 1). The optimization process shows that Aqaba5 received the first choice in the filling order of renewables.

5.4. Multi-point solutions using NSGA

It is not possible to simultaneously optimize a single solution for a MFOM problem. Therefore, the NSGA is applied to give alternative solutions, or what is called Pareto points, in which the Pareto frontier can be obtained.

5.4.1. 2D Pareto Points – AEI vs. ASCE

Fig. 8 shows that the ASCE and the AEI are optimized as a MFOM problem using the NSGA. Increasing the ASCE will gradually decrease the AEI values. Comparing the first and the final point of the Pareto points shows that decreasing the AEI by 32.91% is at the expense of the ASCE, which has been increased by 15.21%.

5.4.2. 2D Pareto Points – AEI vs. RP

Fig. 9 shows another set of trade-offs for MFOM optimized using the NSGA. The RP at the end of the Pareto points is increased around 14.90 times the RP at the first Pareto point. The corresponding reduction of the AEI is 68.26%. This will offer different design alternatives for the decision makers based on specific preferences in their energy plan investment. As can be seen in Fig. 9 more renewable penetration will rapidly reduce the AEI. Therefore, it can be foreseen that a very low-carbon energy production can be achieved in the near future.

5.4.3. 2D Pareto Points – AEI vs. LCOE

Fig. 10 shows another trade-off relationship represented by the Pareto Points for the LCOE and the AEI. Moving from the left to the right side of Fig. 10, i.e from the first to the final point will minimize the AEI by 34.46%, while the LCOE will be maximized by 66.73%.

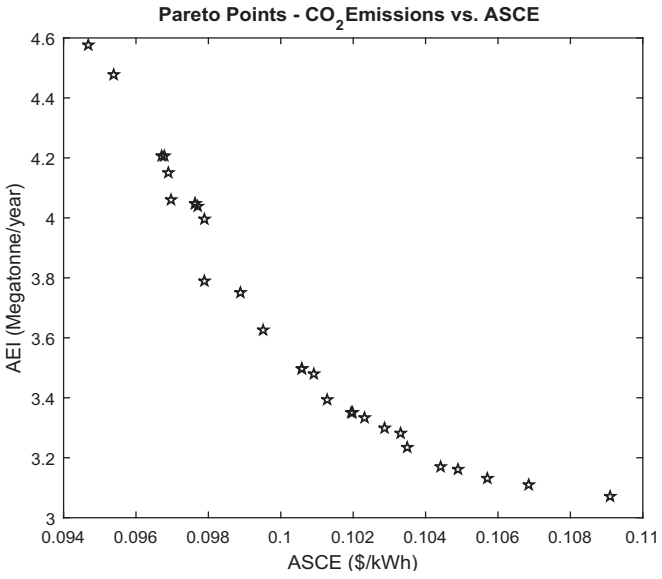

Fig. 8. Pareto points – CO_2 emissions vs. ASCE.

5.4.4. Triple-S procedure - 2D Pareto Frontier

The developed sweet spot selection, the SSS or triple-S procedure helps the decision makers to obtain an excellent solution for

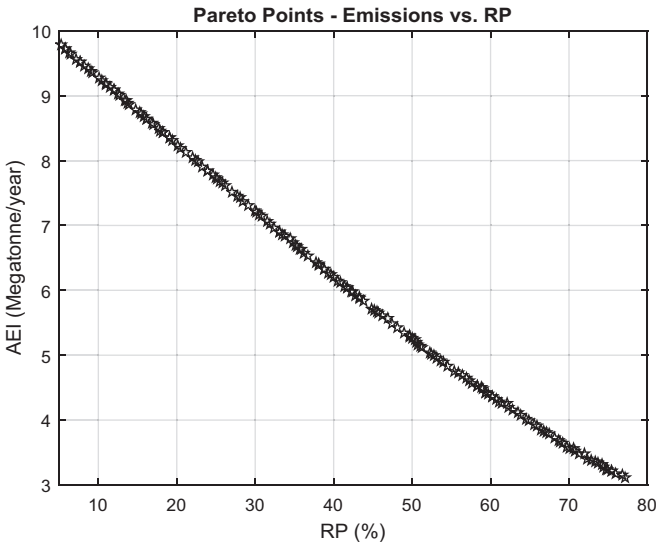

Fig. 9. Pareto points – CO_2 emissions vs. RP.

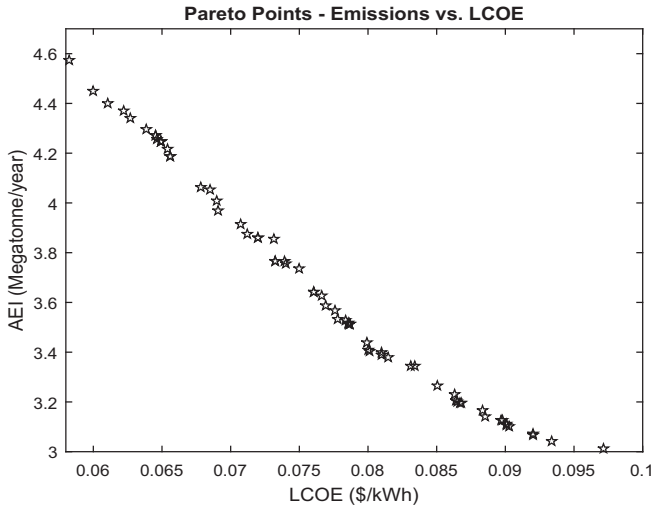

Fig. 10. Pareto points − CO_2 emissions vs. LCOE.

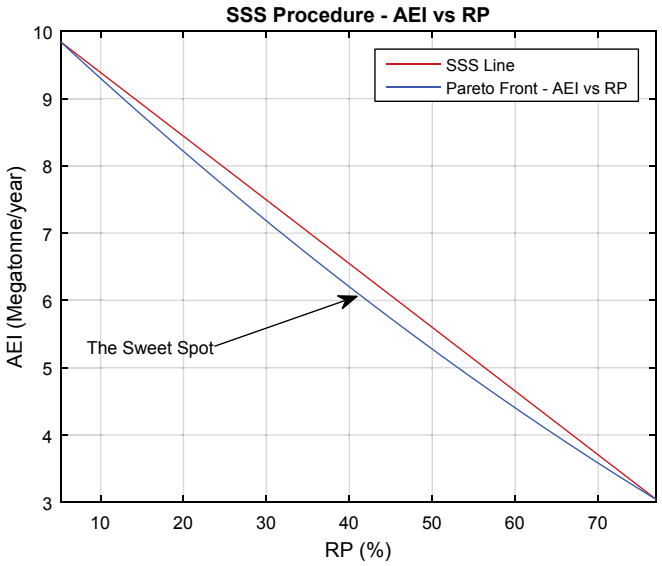

Fig. 12. Triple-S procedure for the Pareto front of Fig. 9.

the two FOMs problems. This helps find the Sweet Spot Point (SSP) as shown in Fig. 11. First, one needs to find the linear triple-S curve function which extends from the first to the last point of the Pareto points of Figs. 8–10. A Pareto front will be obtained for the actual NSGA optimized Pareto points. Thereafter, an iterative technique is applied to find the largest deviation between those two functions. The corresponding SSP for the two FOMs of Fig. 11 is computed to be 3.3762 Megatons/year for the AEI, and 0.1019 $/kWh for the ASCE. Moreover, the application of the triple-S procedure for the Pareto front in Fig. 12 will help get an acceptable solution for the AEI (6.0994 Megatons/year) and the RP (41.0803%). Further, applying the same triple-S procedure for the Pareto front of Fig. 13, helps get a SSP of 0.0808$/kWh for the LCOE, and 3.4288 Megatons/year for the AEI. In all of these three cases, triple-S procedure helps investors find a solution that is acceptable both environmentally and economically.

5.4.5. 3D Pareto Frontier

3D Pareto frontier includes three objectives. It helps visualize the behaviour of the non-dominated solutions in the 3D space. Fig. 14 shows a 3D Pareto front for RP, LCOE and AEI. In the low penetration region, the AEI is very high, because most of the

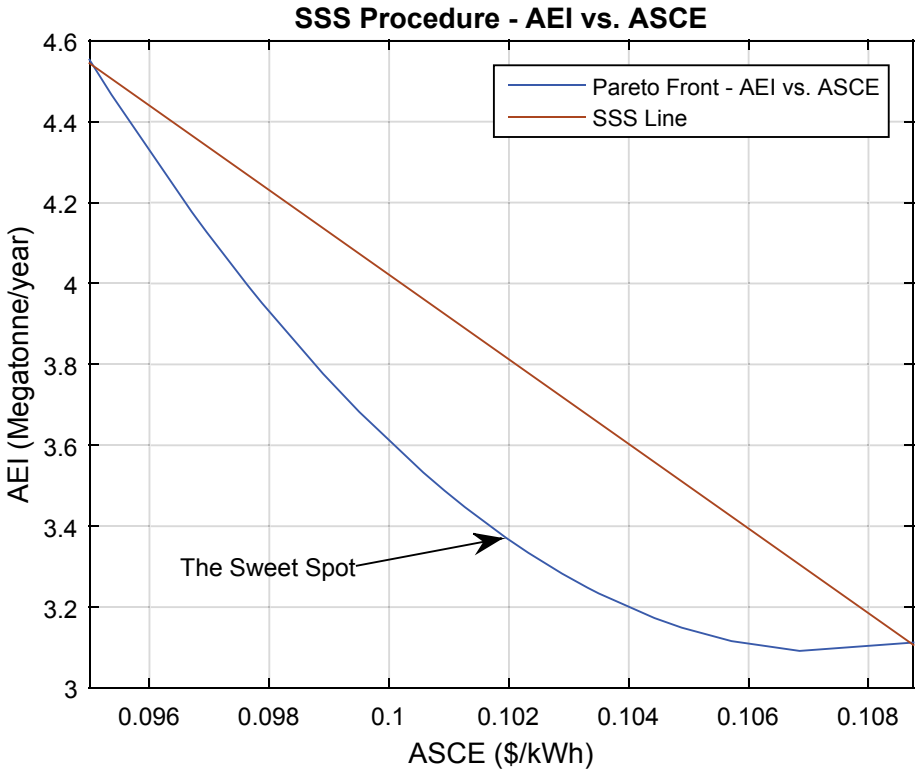

Fig. 11. Triple-S procedure for the Pareto front of Fig. 8.

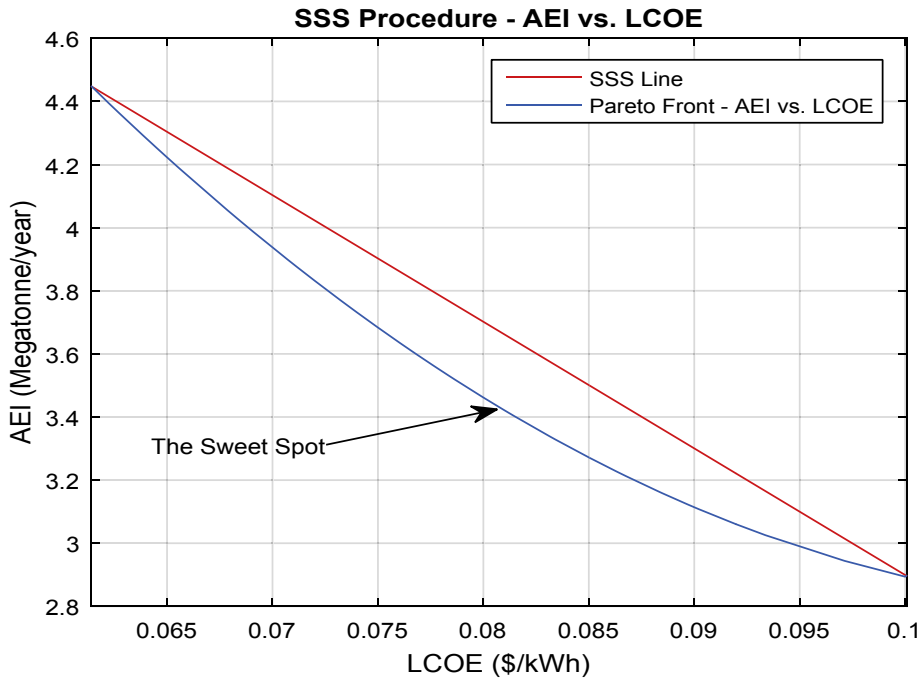

Fig. 13. Triple-S procedure for the Pareto front of Fig. 10.

energy to supply the national load comes from the conventional utility grid regardless the value of the LCOE that is the price of energy produced by renewables. As the RP increases, the AEI is gradually decreases (See Fig. 9). As the RP becomes higher, the LCOE starts affecting the 3D surface. Therefore, to the right of Fig. 14, as the LCOE increases the AEI is gradually reduced as shown in Fig. 10.

6. Uncertainty analysys

Since the results come from simulation, a proper uncertainty analysis is carried out in this paper. The uncertainty analysis is done by applying percentage variations on important parameters. These include, solar irradiance, wind speed and the load demand a well. All uncertainty results in Table 9 are compared to the annual system cost of energy ASCE value optimized before and shown in Table 6.

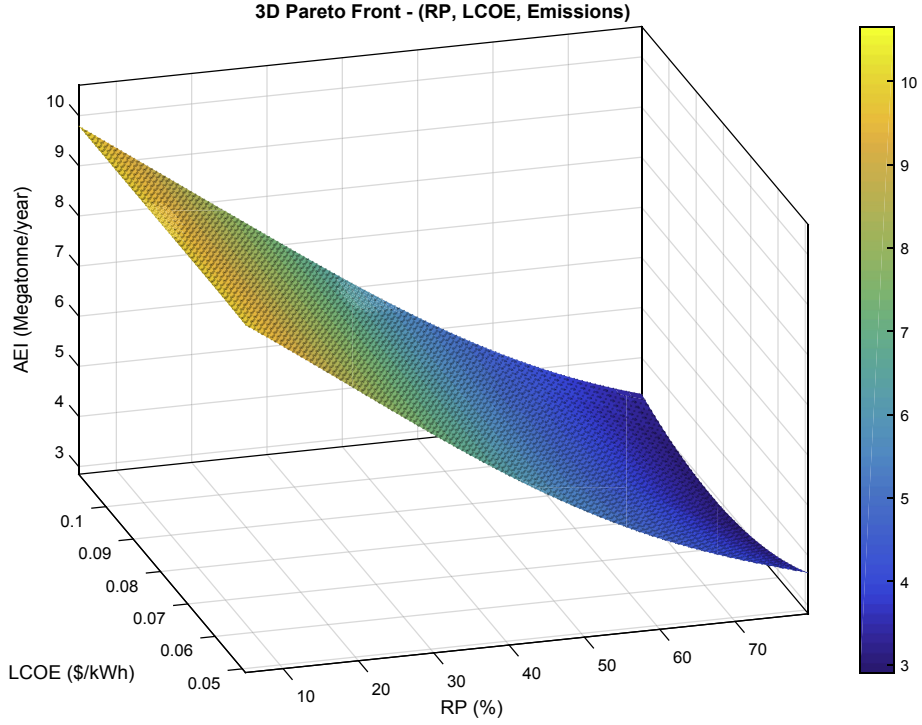

Fig. 14. Pareto front – (RP, LCOE, CO_2 emissions).

Table 9
Uncertainty analysis.

Uncertainty parameter	Uncertainty percentage (%)	ASCE ($/kWh)	Percentage increase/decrease
Solar irradiance	−10	0.1011555	+6.82%
	+10	0.0953964	+0.74%
Wind speed	−10	0.1077916	+13.83%
	+10	0.0834841	−11.84%
Load demand	+10	0.0953336	+0.67%
	+20	0.0964674	+1.87%

Table 9 shows the effects of changing uncertainty parameters on the value of the objective function (or FOM) in our study, which is the ASCE. The ASCE optimal value, corresponding to each uncertainty percentage, is obtained by the GA in our design tool.

It can be noticed that decreasing the hourly wind speed values by 10% increases the ASCE by 13.83% which around two times that in case of decreasing the hourly solar irradiance by the same percentage. This is because wind turbines are cheaper than PV modules as described before in Table 2. This fact has been enhanced when applying 10% uncertainty increase on both solar insolation and wind speeds. As seen in Table 9, that 10% wind speed increase, reduces the ASCE by 11.84%. However, increasing the solar irradiance by the same percentage causes a slightly increase in the ASCE by 0.74%. Finally, the load demand will definitely be increased in the future which will be reflected on the system size and hence the cost. Thereby, increasing the load demand hourly values by 10% and 20% increases the ASCE by 0.67% and 1.87% respectively as shown in Table 9.

7. Conclusion

This paper studies the crucial problem of multipoint connection in order to integrate renewables to a national utility grid system. The case study of Jordan national utility grid is investigated to implement the design procedure, modeling and optimization techniques. Other countries with differing specifics could be other interesting case studies. Wind and solar PV have been combined as multi-point connection taking into account resource availability and grid capacity, to optimize the cost of electrical energy to the end user. In other words, the national electrical load demand of an entire country of Jordan is supplied by finding the optimal configuration in six locations (or cities). Only four cities of higher potential for wind and/or PV energy were used to install wind farms and/or PV arrays, based on their potential priority for installing renewables. The optimal wind and/or PV configuration is found for multiple high potential cities in order to supply the Jordanian national load demand, as a case study. The results show that the hybrid wind/PV is the optimal one at the Aqaba5 site. The wind only is the best for two other cities. The PV only is the optimal to install at the MaanLH site. There is no need to install renewables at the remaining cities for the current national load. This is done by building a new optimization design tool, which is based on the GA to solve a single FOM and a NSGA to solve a MFOM problem. This design tool computes the number of WTs, the number of PVs and the sharing percent of wind and PV in each promising city. For Jordan, the GA optimizes the ASCE as the FOM to be 32.57% less than the fossil fuelled utility grid purchased price. This is an excellent result that indicates the economic feasibility of the optimized system. Results show many other significant figures such as levelized cost of energy (LCOE), total net present cost (TNPC), renewable penetration (RP) and annual emission indicator (AEI), which are 0.058212 $/kWh, $8.713857 billion, 59.49817% and 4.576 Megatonne/year, respectively. The NSGA is used to solve the MFOM problems of AEI vs. ASCE, AEI vs. LCOE, AEI vs. RP and AEI vs. LCOE vs RP. The results are either a 2D or a 3D Pareto frontier. The triple-S procedure is developed to help select the sweet spot in the two FOMs problems. This helps obtain environmental and feasible solutions recommended for investors that are looking to have a single point solution out of a multi-objective problem. Furthermore, because the outcomes obtained from simulation, a proper uncertainty analysis is performed in this study in order to prove the robustness of the designed system and procedure. Several percentage variations are applied on crucial parameters such as solar irradiance, wind speed as well as the load demand.

In sum, the methods described in this paper reduces the actual national sustainable power plant problem to math models and then solving them by various optimization techniques. To summarize, the contributions of this paper are multi-point connection to a national grid, holistic definition and modeling of the engineering and financial problems, optimal design tool solutions to the multi-point connection problem definition and model, suggesting this as a case study of the concept of "local solutions for a global problem." Such a holistic approach is recommended worldwide especially in the developing countries.

Acknowledgement

The authors would like to thank Yarmouk University, Irbid, Jordan, for their support to accomplish this research work.

References

[1] F. Bua, A. Baggini, Overview of standardization of energy efficiency, in: Electrical Energy Efficiency, John Wiley & Sons, Ltd, 2012, pp. 1–8.
[2] D. Newton, Contemporary World Issues : Wind Energy : a Reference Handbook, ABC-CLIO, Santa Barbara, CA, USA, 2014.
[3] T. Senjyu, D. Hayashi, N. Urasaki, T. Funabashi, Optimum configuration for renewable generating systems in residence using genetic algorithm, IEEE Trans. Energy Convers. 21 (2006) 459–466.
[4] H. Yang, W. Zhou, L. Lu, Z. Fang, Optimal sizing method for stand-alone hybrid solar–wind system with LPSP technology by using genetic algorithm, Sol. Energy 82 (4//2008) 354–367.
[5] V. Mytilinou, A.J. Kolios, Techno-economic optimisation of offshore wind farms based on life cycle cost analysis on the UK, Renew. Energy 132 (2019) 439–454.
[6] M. Noussan, R. Roberto, B. Nastasi, Performance indicators of electricity generation at country level—the case of Italy, Energies 11 (2018) 650.
[7] S. Rodrigues, P. Bauer, P.A. Bosman, Multi-objective optimization of wind farm layouts–Complexity, constraint handling and scalability, Renew. Sustain. Energy Rev. 65 (2016) 587–609.
[8] M. Moeini-Aghtaie, A. Abbaspour, M. Fotuhi-Firuzabad, Incorporating large-scale distant wind farms in probabilistic transmission expansion planning—Part I: theory and algorithm, IEEE Trans. Power Syst. 27 (2012) 1585–1593.
[9] A. Arias-Rosales, G. Osorio-Gómez, Wind turbine selection method based on the statistical analysis of nominal specifications for estimating the cost of energy, Appl. Energy 228 (2018) 980–998.
[10] H. M. K. Al-Masri, "reportDevelopment of an Engineering, Economic and Environmental Design Tool for Planetary Scale Sustainable Power Systems,", Ph. D. Dissertation, 2016.
[11] 02/08/2018). National electric power Company (NEPCO). Available: https://goo.gl/A3mLB2
[12] M. Ranaboldo, B. Domenech, G.A. Reyes, L. Ferrer-Martí, R. Pastor Moreno, A. García-Villoria, Off-grid community electrification projects based on wind and solar energies: a case study in Nicaragua, Sol. Energy 117 (2015) 268–281.

[13] H.M. Al-Masri, M. Ehsani, Feasibility investigation of a hybrid on-grid wind photovoltaic retrofitting system, IEEE Trans. Ind. Appl. 52 (2016) 1979–1988.
[14] A.N. Khan, P. Akhter, G.M. Mufti, Techno-economic evaluation of the centralized hybrid renewable energy systems for off-grid rural electrification, Int. J. Smart Home 10 (2016) 61–68.
[15] H. Al-Masri, M. Ehsani, Feasibility investigation of a hybrid on-grid wind photovoltaic retrofitting system, in: Industry Applications Society Annual Meeting, 2015 IEEE, Addison, TX, 2015, pp. 1–7.
[16] M.R. Patel, Wind and Solar Power Systems : Design, Analysis, and Operation, Taylor & Francis, Boca Raton, FL, 2006.
[17] H.M.K. Al-Masri, A.A. Almehizia, M. Ehsani, Accurate wind turbine annual energy computation by advanced modeling, IEEE Trans. Ind. Appl. 53 (2017) 1761–1768.
[18] M. Cavcar, The International Standard Atmosphere (Isa), vol. 30, Anadolu University, Turkey, 2000.
[19] L. Battisti, Wind Turbines in Cold Climates : Icing Impacts and Mitigation Systems, Springer, Cham ; New York, 2015.
[20] S. Mathew, Wind Energy: Fundamentals, Resource Analysis and Economics, vol. 1, Springer, 2006.
[21] M. Thomson, D.G. Infield, Impact of widespread photovoltaics generation on distribution systems, IET Renew. Power Gener. 1 (2007) 33–40.
[22] E. Skoplaki, A.G. Boudouvis, J.A. Palyvos, A simple correlation for the operating temperature of photovoltaic modules of arbitrary mounting, Sol. Energy Mater. Sol. Cell. 92 (11//2008) 1393–1402.
[23] N. A. Azli, Z. Salam, A. Jusoh, M. Facta, B. C. Lim, and S. Hossain, "Effect of fill factor on the MPPT performance of a grid-connected inverter under Malaysian conditions," in Power and Energy Conference, 2008. PECon 2008. IEEE 2nd International, 2008, pp. 460-462.
[24] D. G. F. Sonnenenergie, Planning and Installing Photovoltaic Systems: a Guide for Installers, architects and engineers: Earthscan, 2007.
[25] EPA). (02/01/2016). Global greenhouse gas emissions data. Available: http://goo.gl/SYIJ5F
[26] M. Brander, A. Sood, C. Wylie, A. Haughton, J. Lovell, Electricity-specific Emission Factors for Grid Electricity, 2011.
[27] A. ROCAMORA and A. AMELLINA. (08/05/2018). IGES list of grid emission factors. Available: https://goo.gl/Jj3mTV
[28] R. Luna-Rubio, M. Trejo-Perea, D. Vargas-Vázquez, G.J. Ríos-Moreno, Optimal sizing of renewable hybrids energy systems: a review of methodologies, Sol. Energy 86 (4//2012) 1077–1088.
[29] M. Mitchell, An Introduction to Genetic Algorithms, MIT press, 1998.
[30] F.-A. Fortin, M. Parizeau, Revisiting the NSGA-II crowding-distance computation, in: Proceedings of the 15th Annual Conference on Genetic and Evolutionary Computation, 2013, pp. 623–630.
[31] H. Fang, Q. Wang, Y. Tu, M. Horstemeyer, An efficient non-dominated sorting method for evolutionary algorithms, Evol. Comput. 16 (2008) 355–384.
[32] G. Ruhe, Y. Zhang, Search Based Software Engineering: 5th International Symposium, SSBSE 2013, St. Petersburg, Russia, August 24-26, 2013. Proceedings, vol. 8084, Springer, 2013.
[33] 08/06/2016). The global carbon atlas Available: http://www.globalcarbonatlas.org/?q=en/emissions